Liver Cancer

Research Article

Liver Cancer 2023;12:262–276
DOI: 10.1159/000528034

Received: June 16, 2022
Accepted: October 2, 2022
Published online: November 28, 2022

Tumor Radiomic Features on Pretreatment MRI to Predict Response to Lenvatinib plus an Anti-PD-1 Antibody in Advanced Hepatocellular Carcinoma: A Multicenter Study

Bin Xu[a] San-Yuan Dong[b] Xue-Li Bai[c] Tian-Qiang Song[d] Bo-Heng Zhang[e] Le-Du Zhou[f] Yong-Jun Chen[g] Zhi-Ming Zeng[h] Kui Wang[i] Hai-Tao Zhao[j] Na Lu[c] Wei Zhang[d] Xu-Bin Li[k] Su-Su Zheng[e] Guo Long[f] Yu-Chen Yang[g] Hua-Sheng Huang[h] Lan-Qing Huang[i] Yun-Chao Wang[j] Fei Liang[l] Xiao-Dong Zhu[a] Cheng Huang[a] Ying-Hao Shen[a] Jian Zhou[a] Meng-Su Zeng[b] Jia Fan[a] Sheng-Xiang Rao[b] Hui-Chuan Sun[a]

[a]Department of Liver Surgery and Transplantation, Liver Cancer Institute and Zhongshan Hospital, Fudan University, Shanghai, China; [b]Department of Radiology, Zhongshan Hospital, Fudan University, Shanghai Institute of Medical Imaging, Shanghai, China; [c]Department of Hepatobiliary and Pancreatic Surgery, The First Affiliated Hospital, Zhejiang University School of Medicine, Hangzhou, China; [d]Department of Hepatobiliary, National Clinical Research Center of Cancer, Oncology Key Laboratory of Cancer Prevention and Therapy, Tianjin Medical University Cancer Institute and Hospital, Tianjin, China; [e]Department of Hepatic Oncology, Xiamen Branch, Zhongshan Hospital, Fudan University, Xiamen, China; [f]Department of General Surgery, Xiangya Hospital, Central South University, Changsha, China; [g]Department of Hepatobiliary Surgery, Ruijin Hospital, Shanghai Jiao Tong University School of Medicine, Shanghai, China; [h]Department of Medical Oncology, The First Affiliated Hospital of Guangxi Medical University, Nanning, China; [i]Department of Hepatic Surgery II, Eastern Hepatobiliary Surgery Hospital, Navy Medical University, Shanghai, China; [j]Department of Liver Surgery, Peking Union Medical College Hospital, Chinese Academy of Medical Sciences and Peking Union Medical College, Beijing, China; [k]Department of Radiology, National Clinical Research Center of Cancer, Tianjin Medical University Cancer Institute and Hospital, Tianjin, China; [l]Department of Biostatistics, Zhongshan Hospital, Fudan University, Shanghai, China

Keywords
Anti-PD-1 antibody · Hepatocellular carcinoma · Lenvatinib · Prediction · Radiomics

Abstract

Introduction: Lenvatinib plus an anti-PD-1 antibody has shown promising antitumor effects in patients with advanced hepatocellular carcinoma (HCC), but with clinical benefit limited to a subset of patients. We developed and validated a radiomic-based model to predict objective response to this combination therapy in advanced HCC patients. ***Methods:*** Patients ($N = 170$) who received first-line combination therapy with lenvatinib plus an anti-PD-1 antibody were retrospectively enrolled from 9 Chinese centers; 124 and 46 into the training and validation cohorts, respectively. Radiomic features were extracted from pretreatment contrast-enhanced MRI. After feature selection, clinicopathologic, radiomic, and clinicopathologic-radiomic models were built using a neural network. The performance of models, incremental predictive value of radiomic features compared with clinicopathologic features and relationship between radiomic features and survivals were assessed. ***Results:*** The clinicopathologic model modestly predicted objective response

Bin Xu and San-Yuan Dong contributed equally to this work.

Karger@karger.com
www.karger.com/lic

Correspondence to:
Sheng-Xiang Rao, raoxray@163.com
Hui-Chuan Sun, sun.huichuan@zs-hospital.sh.cn

with an AUC of 0.748 (95% CI: 0.656–0.840) and 0.702 (95% CI: 0.547–0.884) in the training and validation cohorts, respectively. The radiomic model predicted response with an AUC of 0.886 (95% CI: 0.815–0.957) and 0.820 (95% CI: 0.648–0.984), respectively, with good calibration and clinical utility. The incremental predictive value of radiomic features to clinicopathologic features was confirmed with a net reclassification index of 47.9% ($p < 0.001$) and 41.5% ($p = 0.025$) in the training and validation cohorts, respectively. Furthermore, radiomic features were associated with overall survival and progression-free survival both in the training and validation cohorts, but modified albumin-bilirubin grade and neutrophil-to-lymphocyte ratio were not. ***Conclusion:*** Radiomic features extracted from pretreatment MRI can predict individualized objective response to combination therapy with lenvatinib plus an anti-PD-1 antibody in patients with unresectable or advanced HCC, provide incremental predictive value over clinicopathologic features, and are associated with overall survival and progression-free survival after initiation of this combination regimen.

Introduction

Hepatocellular carcinoma (HCC) is one of the most prevalent malignant tumors and one of the leading causes of cancer mortality in the world and China [1, 2]. Most patients with HCC are diagnosed at an advanced stage, non-amenable to curative treatment [3].

In recent years, combination strategies including targeted therapy plus immunotherapy, such as atezolizumab plus bevacizumab and sintilimab plus a bevacizumab biosimilar [4], have been approved for the first-line treatment of advanced HCC (the latter only in China). Furthermore, combination therapy with lenvatinib plus pembrolizumab for the first-line treatment in advanced HCC was investigated in a phase Ib trial (KEYNOTE-524 study) and showed a promising objective response rate (ORR) of 36% (according to Response Evaluation Criteria in Solid Tumors, version 1.1 (RECIST v1.1)), with promising progression-free survival (PFS) and overall survival (OS) [5]. Similar ORRs have been reported for lenvatinib in combination with a range of different anti-programmed cell death protein 1 (PD-1) antibodies [6]. Although LEAP-002 study (lenvatinib plus pembrolizumab vs. lenvatinib as first-line therapy for advanced HCC, NCT03713593) is a negative trial in terms of PFS and OS, it is also noted that ORR was much higher in the combination arm than the lenvatinib monotherapy arm [7], which implies there may be a role of this combination therapy in neoadjuvant therapy. Indeed, preliminary investigation suggested a great value of this combination treatment in either conversion therapy or neoadjuvant therapy settings [8–10]. A multicenter prospective clinical trial has been initiated in China to further investigate the efficacy of this combination in the neoadjuvant setting (NCT05389527). Therefore, it is also important to predict efficacy of this combination therapy, especially in the neoadjuvant setting when we already have multiple choices for systemic therapies.

Although the combination of lenvatinib plus an anti-PD-1 antibody provides a relatively high ORR, the clinical benefit is limited to a subset of patients. As the incidence of grade 3/4 adverse events is ~50% with this combination [5, 11], identifying patients who are more likely to respond before initiating treatment is of clinical significance. However, currently, no validated biomarker has been identified to predict the response to combination therapy with targeted therapy plus immunotherapy [12].

Biomarkers such as programmed death-ligand 1 (PD-L1) expression, tumor mutational burden, microsatellite instability [13], and mismatch repair deficiency [14] have been proposed to predict response to immunotherapy in HCC and other cancers. However, whether these biomarkers could predict the efficacy of combination treatment with targeted therapy plus immunotherapy remains unclear [12]. Furthermore, these are tissue-based biomarkers that require invasive biopsies or procedures to obtain tumor tissue samples and do not adequately characterize the spatial and temporal heterogeneity of tumors.

Radiomics is an emerging field that converts standard-of-care medical imaging into high-throughput, mineable, and quantitative features using a variety of predefined image-characterization algorithms [15, 16]. Medical images contain information that directly reflects the overall tumor burden and each tumor lesion [16]. Therefore, radiomics, which can be perceived as a "digital biopsy" of the entire tumor, provides a noninvasive, repeatable, and comprehensive view of tumor biology and heterogeneity, without the need for additional blood or tissue samples.

Radiomics have been shown to improve diagnostic [17], prognostic [18, 19], and predictive accuracy [20, 21] in HCC. Radiomics can also be used to predict response to transcatheter arterial chemoembolization (TACE) in HCC [22], neoadjuvant therapy in rectal and breast

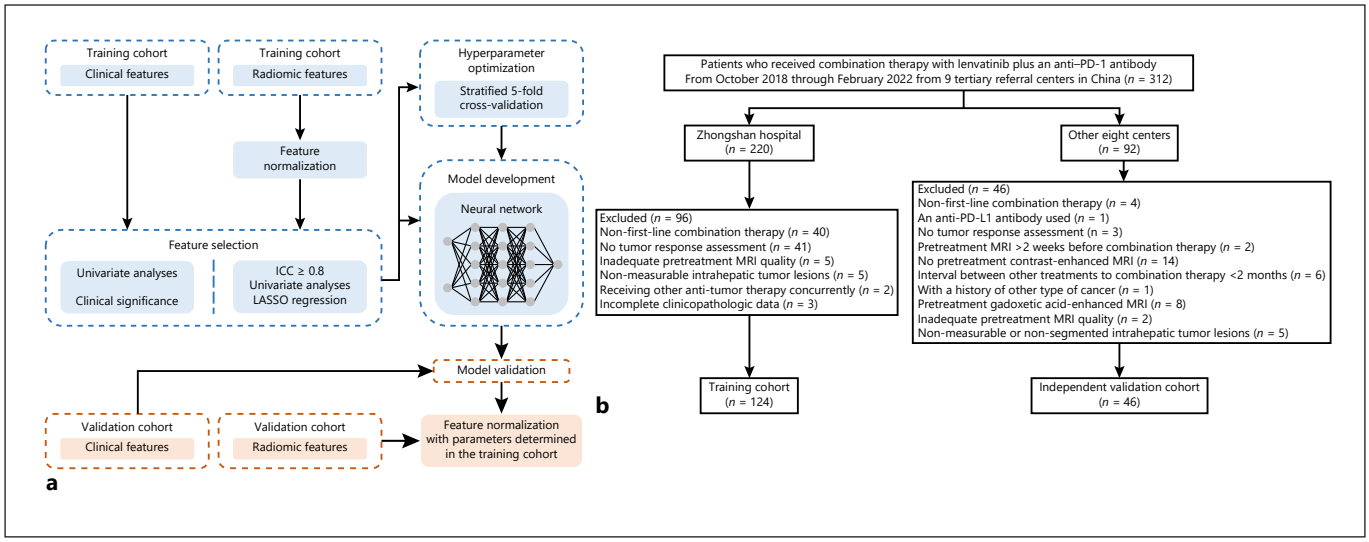

Fig. 1. Framework and flowchart for this study. **a** Framework for development and validation of prediction models. **b** Flowchart of patient enrollment and grouping. ICC, intraclass correlation coefficient; LASSO, least absolute shrinkage and selection operator; MRI, magnetic resonance imaging; PD-1, programmed cell death protein 1; PD-L1, programmed cell death-ligand 1.

cancer [23, 24], systemic therapy in lung cancer [25], and to immune checkpoint inhibitors in solid tumors [26, 27]. However, to the best of our knowledge, no study has investigated the ability of radiomics to predict response to lenvatinib plus an anti-PD-1 antibody in advanced HCC.

Magnetic resonance imaging (MRI) provides a higher soft-tissue contrast than computed tomography (CT) images, and contrast-enhanced MRI remains the most reliable radiologic technique to evaluate response to systemic therapy in HCC [28]. Therefore, we hypothesized that a radiomic model to predict response to lenvatinib plus an anti-PD-1 antibody in unresectable or advanced HCC based on pretreatment contrast-enhanced MRI would have similar or incremental value to a clinicopathologic model. In this study, we aimed to develop a radiomic model based on pretreatment contrast-enhanced MRI to predict objective response to the first-line combination therapy with lenvatinib plus an anti-PD-1 antibody in patients with unresectable or advanced HCC, and validate this radiomic model using a multicenter dataset.

Materials and Methods

Study Design and Patients

This was a retrospective, multicenter study involving 9 tertiary referral centers in China. Consecutive patients diagnosed with HCC according to local and international guidelines [29, 30] were eligible for inclusion if they received combination therapy with lenvatinib plus an anti-PD-1 antibody (see online suppl. methods for details of treatment; see online suppl. Result S1, online suppl. Table S9 and online suppl. Table S10 for details of treatment-related adverse events; for all online suppl. material, see www.karger.com/doi/10.1159/000528034) as a first-line systemic treatment between October 2018 and February 2022, had undergone a pretreatment contrast-enhanced MRI within 2 weeks before initiating combination therapy, and had tumor response assessments every 2 months (±2 weeks) via CT or MRI according to RECIST v1.1. Patients were also required to have an interval of at least 2 months between any previous therapy (e.g., TACE, radiofrequency ablation, hepatectomy) and the initiation of combination therapy, and have at least one tumor response assessment after initiating combination therapy. Different anti-PD-1 antibodies were permitted across the study population to reflect real-world practice more accurately and showed similar ORRs when combined with lenvatinib [6]. Exclusion criteria were incomplete clinicopathologic data; a history of cancer other than HCC; a gadoxetic acid-enhanced pretreatment MRI; inadequate MRI quality; intrahepatic tumor lesions that could not be measured or segmented in magnetic resonance (MR) images; and additional antitumor treatment after the initiation of combination therapy.

Eligible patients formed two cohorts: a training cohort recruited from an ongoing observational, prospective cohort study (NCT04639284) at one of the centers (Zhongshan Hospital, Fudan University), whose data were used to build the model; and an independent validation cohort recruited from the remaining 8 centers (online suppl. methods).

Objective and Sample Size

The objective of this study was to predict objective response (defined as a complete response or partial response as the best overall response) to the first-line combination therapy with lenvatinib plus an anti-PD-1 antibody with an area under the receiver operating characteristic (ROC) curve (AUC) of ≥0.8.

Table 1. Baseline characteristics of patients in the training cohort and independent validation cohort

Variables	Training cohort (n = 124)	Validation cohort (n = 46)	p value
Age in years, mean±SD	55.37±11.2	56.96±11.13	0.412
Sex			
Female	10 (8.1)	6 (13.0)	0.377
Male	114 (91.9)	40 (87.0)	
ECOG PS			
0	65 (52.4)	35 (76.1)	0.010
1	50 (40.3)	11 (23.9)	
2	9 (7.3)	0 (0)	
Child-Pugh class			
A	116 (93.5)	43 (93.5)	1
B	8 (6.5)	3 (6.5)	
HBsAg			
Negative	28 (22.6)	13 (28.3)	0.570
Positive	96 (77.4)	33 (71.7)	
HBV DNA			
≤10^3/mL	72 (58.1)	33 (71.7)	0.146
>10^3/mL	52 (41.9)	13 (28.3)	
BCLC stage			
0	2 (1.6)	0 (0)	0.942
A	15 (12.1)	4 (8.7)	
B	22 (17.7)	9 (19.6)	
C	85 (68.5)	33 (71.7)	
CNLC stage			
Ia	2 (1.6)	3 (6.5)	0.413
Ib	8 (6.5)	2 (4.3)	
IIa	3 (2.4)	2 (4.3)	
IIb	25 (20.2)	6 (13.0)	
IIIa	48 (38.7)	16 (34.8)	
IIIb	38 (30.6)	17 (37.0)	
Macrovascular invasion			
No	58 (46.8)	22 (47.8)	1
Yes	66 (53.2)	24 (52.2)	
Extrahepatic disease			
No	86 (69.4)	29 (63.0)	0.551
Yes	38 (30.6)	17 (37.0)	
AFP, ng/mL	784 (21.85, 12512.25)	390 (25.95, 1481.5)	0.170
AFP			
≤400 ng/mL	51 (41.1)	23 (50.0)	0.389
>400 ng/mL	73 (58.9)	23 (50.0)	
Sum of diameter of baseline intrahepatic target lesions, cm	11.45 (5.57, 15)	9.91 (5.85, 12.46)	0.188
Anti-PD-1 antibody used			
Camrelizumab	42 (33.9)	13 (28.3)	0.724
Nivolumab	4 (3.2)	0 (0)	
Pembrolizumab	11 (8.9)	4 (8.7)	
Sintilimab	47 (37.9)	18 (39.1)	
Tislelizumab	9 (7.3)	6 (13)	
Toripalimab	11 (8.9)	5 (10.9)	
Tumor objective response			
No	87 (70.2)	33 (71.7)	0.991
Yes	37 (29.8)	13 (28.3)	

Table 1 (continued)

Variables	Training cohort (n = 124)	Validation cohort (n = 46)	p value
Tumor response			
CR	5 (4)	1 (2.2)	0.942
PR	32 (25.8)	12 (26.1)	
SD	67 (54)	27 (58.7)	
PD	20 (16.1)	6 (13.0)	
Progressive disease			
No	104 (83.9)	40 (87.0)	0.797
Yes	20 (16.1)	6 (13.0)	

Data are n (%) or median (IQR) unless indicated otherwise. AFP, α-fetoprotein; BCLC, Barcelona Clinic Liver Cancer; CNLC, China Liver Cancer; CR, complete response; ECOG PS, Eastern Cooperative Oncology Group performance status; HBV DNA, hepatitis B virus DNA copy number; HBsAg, hepatitis B surface antigen; IQR, interquartile range; PD, progressive disease; PD-1, programmed cell death protein 1; PR, partial response; SD, stable disease.

Table 2. Univariate logistic regression analyses of clinicopathologic features in the training cohort between patients with and without an objective response

Features	Odds ratio	95% CI	p value
Age in years (divided by 5)	1.042	0.876–1.242	0.644
Sex			
Male versus female	1.772	0.418–12.142	0.483
ECOG PS			
1 versus 0	0.862	0.385–1.886	0.713
2 versus 0	0.653	0.094–2.865	0.606
Child-Pugh class			
B versus A	1.447	0.284–6.235	0.626
HBsAg			
Positive versus negative	0.704	0.292–1.764	0.441
HBV DNA			
$>10^3$/mL versus $\leq 10^3$/mL	0.397	0.165–0.896	0.031
BCLC stage			
A versus 0	0.837	0.22–2.652	0.775
B versus 0	0.859	0.286–2.31	0.772
C versus 0	1.350	0.588–3.272	0.490
Macrovascular invasion			
Yes versus no	0.770	0.354–1.666	0.506
Extrahepatic disease			
Yes versus no	1.897	0.837–4.275	0.122
AFP in ng/mL (divided by 100)	0.999	0.997–1.001	0.514
AFP			
>400 ng/mL versus ≤400 ng/mL	0.471	0.213–1.025	0.059
Sum of diameter of baseline intrahepatic target lesions in cm	0.978	0.913–1.047	0.529

AFP, α-fetoprotein; BCLC, Barcelona Clinic Liver Cancer; CI, confidence interval; ECOG PS, Eastern Cooperative Oncology Group performance status; HBV DNA, hepatitis B virus DNA copy number; HBsAg, hepatitis B surface antigen.

To avoid model overfitting, the rule of thumb is that the number of predictors should remain within 1/20-1/6 of the sample size in the training cohort used to build a model [31]. A sample size of at least 33 patients (10 patients with objective responses and 23 patients without objective responses) in each cohort was required based on the following assumption: a power of 0.8, two-sided α of 0.05, alternative hypothesis of an AUC of 0.8 compared with the null hypothesis of an AUC of 0.5, and an

Table 3. ROC analyses of prediction models

	AUC (95% CI)[a]	Cut-off	Numerator/denominator (%)				
			Acc	Sens	Spec	PPV	NPV
Clinicopathologic model							
Training cohort	0.748 (0.656–0.840)	0.614	105/124 (84.7)	18/37 (48.6)	87/87 (100)	18/18 (100)	87/106 (82.1)
Validation cohort	0.702 (0.547–0.884)		33/46 (71.7)	4/13 (30.8)	29/33 (87.9)	4/8 (50.0)	29/38 (76.3)
Radiomic model							
Training cohort	0.886 (0.815–0.957)	0.504	114/124 (91.9)	30/37 (81.1)	84/87 (96.6)	30/33 (90.9)	84/91 (92.3)
Validation cohort	0.820 (0.648–0.984)		40/46 (87.0)	8/13 (61.5)	32/33 (97.0)	8/9 (88.9)	32/37 (86.5)
Clinicopathologic-radiomic model							
Training cohort	0.987 (0.968–1.000)	0.443	121/124 (97.6)	37/37 (100)	84/87 (96.6)	37/40 (92.5)	84/84 (100)
Validation cohort	0.876 (0.750–1.000)		39/46 (84.8)	9/13 (69.2)	30/33 (90.9)	9/12 (75.0)	30/34 (88.2)

Acc, accuracy; AUC, area under the receiver operating characteristic curve; CI, confidence interval; NPV, negative predictive value; PPV, positive predictive value; Sens, sensitivity; Spec, specificity. [a]Calculated with bootstrap resampling (n = 1,000).

Table 4. Relationship between the observed and predicted response to combination therapy

	Observed response			p value
	predicted response	objective response	no objective response	
Radiomic model				
Training cohort	Objective response	30 (90.9)	3 (9.1)	<0.001
	No objective response	7 (7.7)	84 (92.3)	
Validation cohort	Objective response	8 (88.9)	1 (11.1)	<0.001
	No objective response	5 (13.5)	32 (86.5)	
Clinicopathologic-radiomic model				
Training cohort	Objective response	37 (92.5)	3 (7.5)	<0.001
	No objective response	0 (0)	84 (100)	
Validation cohort	Objective response	9 (75.0)	3 (25.0)	<0.001
	No objective response	4 (11.8)	30 (88.2)	

Data were expressed as n (%).

expected ORR of ~30% based on a previous report [6]. Sample size was calculated using PASS 2021 (NCSS, LLC, Kaysville, UT, USA).

Radiomic Feature Analysis

Image Acquisition

MRI data acquisition and scan parameters are described in online supplementary methods and online supplementary Table S1, respectively.

Image Segmentation

Tumor segmentation was performed using 3D slicer (version 4.11). The regions of interest for all intrahepatic target tumors were manually drawn along the tumor boundary on arterial phase and delayed phase images by a radiologist (S-Y Dong), and 60 randomly selected tumors were re-segmented by a senior radiologist (S-X Rao) to test the robustness and reproducibility of extracted radiomic features. Both radiologists were blinded to clinical, laboratory, and response assessment results for all patients. A representative case of tumor contouring on MR images is shown in online supplementary Figure S1.

Radiomic Feature Extraction

Image preprocessing and radiomic feature extraction were performed using PyRadiomics (v3.0.1) [32]. Briefly, MRI signal intensity was normalized followed by resampling and interpolation of voxels to minimize the effects of different MRI acquisition parameters and scanners, which are detailed in the online supplementary methods. Finally, 1,118 features were extracted for each of the arterial and delayed phases (2,236 in total). The extracted features in each image type are listed in online supplementary Table S2.

Robustness, Reproducibility, and Normalization

Radiomic features with an interobserver intraclass correlation coefficient (ICC) <0.8 were excluded to ensure robustness and

reproducibility as previously reported [31] and were normalized using z-score method.

Prediction Model Development and Validation

The framework for the development and validation of the predictive models is shown in Figure 1a.

Feature Selection

Clinicopathologic features with a p value <0.2 in univariate logistic regression analyses along with features that may have clinical significance [33] were selected to build a clinicopathologic model. Radiomic features with an interobserver ICC ≥0.8 and a p value <0.1 in Student's t test were selected by least absolute shrinkage and selection operator logistic regression with stratified 5-fold cross-validation, maximizing the AUC, to build a radiomic model. The features in the clinicopathologic model and the radiomic score (rad-score) calculated using the radiomic model was used to build the clinicopathologic-radiomic model.

Prediction Model Building

All prediction models were built using a neural network model in the training cohort. To avoid overfitting and increase generalizability, hyperparameter optimization was performed. The neural network model and hyperparameter optimization are described in the online supplementary methods. The prediction models were validated in the independent validation cohort to assess generalizability following development in the training cohort.

Model Performance Assessment

Bootstrap resampling (n = 1,000) was used to calculate an AUC with 95% confidence intervals (CI) and compare the difference between two ROCs. The optimal cut-off threshold of prediction models was determined using ROC by maximizing the Youden index in the training cohort. Net reclassification index (NRI) was used to quantify how well a new model reclassifies patients compared with an old model, at their respective cut-off values, which is particularly useful if there is no significant difference between the AUCs for the new and old models [34]. A NRI >0 indicates the predictive ability of the new model is better than that of old model. Calibration curves were plotted to assess the calibration of models. Decision curve analysis was conducted to determine the clinical utility of the prediction models by quantifying the net benefits at different threshold values [35].

Follow-Up

Patients were followed every 60 days (±7 days) after initiation of combination therapy. OS was calculated from the date of first dose of drug to death from any cause or censored on the last follow-up. PFS was calculated from the date of first dose of drug to the first documented disease progression or death from any cause.

Statistical Analysis

Categorical variables were expressed as counts and percentages, and were compared using Pearson's χ^2 analysis, Fisher's exact test, or Mann-Whitney U test, as appropriate. Continuous variables were expressed as mean (± standard deviation) or median (interquartile range (IQR)) and were compared using Student's t test or Mann-Whitney U test, as appropriate. The multivariate logistic regression was used to identify independent predictors. Survival curves were calculated using the Kaplan-Meier method and compared using the log-rank test. A p value <0.05 was considered statistically significant. All statistical analyses were performed using the R software (version 4.1.2; packages used listed in online suppl. Table S3).

Results

Patient Characteristics

In total, 170 eligible patients were enrolled, 124 in the training cohort and 46 in the independent validation cohort (Fig. 1b). Patients in the validation cohort had better Eastern Cooperative Oncology Group performance status than patients in the training cohort (p = 0.010); there were no significant differences in other baseline demographic and disease characteristics between the training and validation cohorts (Table 1). The ORRs were 29.8% (37/124) and 28.3% (13/46) in the training and validation cohorts, respectively (p = 0.991).

The baseline demographic and disease characteristics of patients with and without an objective response in the training and validation cohorts are summarized in online supplementary Tables S4 and S5. In the training cohort, a smaller proportion of patients who had an objective response had a hepatitis B virus DNA copy number $>10^3$/mL compared with those who did not have an objective response (27.0% vs. 48.3%, p = 0.046). Patients who had an objective response also had lower baseline α-fetoprotein (AFP, ng/mL) levels than those who did not have an objective response (median (IQR), 80.4 (5.5–10,385) vs. 1,104 (74.85–14,559), p = 0.029). In the validation cohort, patients with an objective response had a higher proportion of an Eastern Cooperative Oncology Group performance status of 0 (100% vs. 66.7%, p = 0.020) and a lower proportion of AFP >400 ng/mL (23.1% vs. 60.6%, p = 0.049) than those without an objective response.

Association between Clinicopathologic Features and Objective Tumor Response

Clinicopathologic features with a p value <0.2 in univariate logistic regression analyses in the training cohort were hepatitis B virus DNA ($>10^3$/mL vs. $\leq 10^3$/mL), extrahepatic disease (yes vs. no), and AFP (>400 ng/mL vs. ≤400 ng/mL) (Table 2). The additional features that may have clinical significance in predicting objective response were macrovascular invasion (yes vs. no), and sum of diameter of baseline intrahepatic target lesions in cm. The continuous form of AFP was used instead as the continuous form can provide more information than the categorical form.

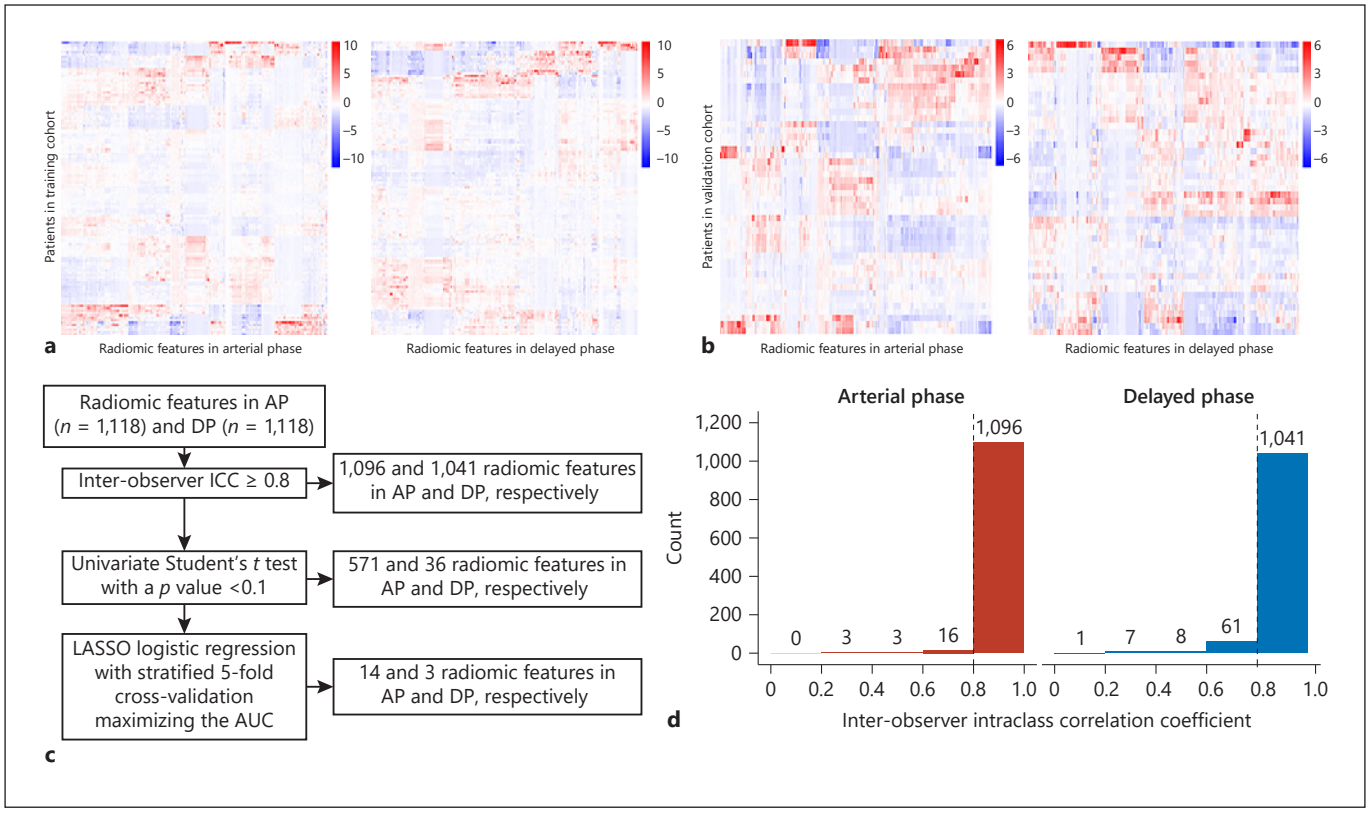

Fig. 2. Heatmap expression of radiomic features and feature selection. **a**, **b** Heatmap expression of radiomic features extracted from the arterial and delayed phase of the pretreatment MRI in the training cohort and validation cohort, respectively. **c** Radiomic feature selection for prediction of objective response to combination therapy in the training cohort. The distribution of ICC of radiomic features in the arterial and delayed phases are shown in Figure 2d. **d** The distribution of ICC of radiomic features in the arterial and delayed phases in the training cohort. AP, arterial phase; AUC, area under the receiver operating characteristic curve; DP, delayed phase; ICC, intraclass correlation coefficient; LASSO, least absolute shrinkage and selection operator.

The clinicopathologic model was built with 1, 4, and 2 neurons in hidden layers 1, 2, and 3, respectively. The diagram and formula of this model are shown in online supplementary Figure S2. The AUC (95% CI) using this model was 0.748 (0.656–0.840) and 0.702 (0.547–0.884) in the training and validation cohorts, respectively, after bootstrap resampling (n = 1,000) (online suppl. Fig. S3). The optimal cut-off threshold for this model was 0.614; accuracy, sensitivity, specificity, positive predictive value (PPV), and negative predictive value (NPV) for this model are summarized in Table 3. These results indicated that clinicopathologic features modestly predict the objective response to lenvatinib plus an anti-PD-1 antibody. Furthermore, the training and validation cohorts did not meet the study objective in the clinicopathologic model.

Radiomic Features Predicted the Objective Tumor Response

The heatmap expressions of extracted radiomic features in each patient are shown in Figure 2a, b. The details of radiomic feature selection and selected features are described in Figure 2c and online supplementary Result S2, respectively. Ultimately, 14 radiomic features selected in the arterial and 3 in the delayed phase were used to build the radiomic model.

The radiomic model was built with 2 neurons in the single hidden layer. The diagram and formula of this model are shown in online supplementary Figure S4. The AUC (95% CI) using this model was 0.886 (0.815–0.957) and 0.820 (0.648–0.984) in the training and validation cohorts, respectively, after bootstrap resampling (n = 1,000) (Fig. 3a). The rad-score was identified as an independent predictor for objective response in both

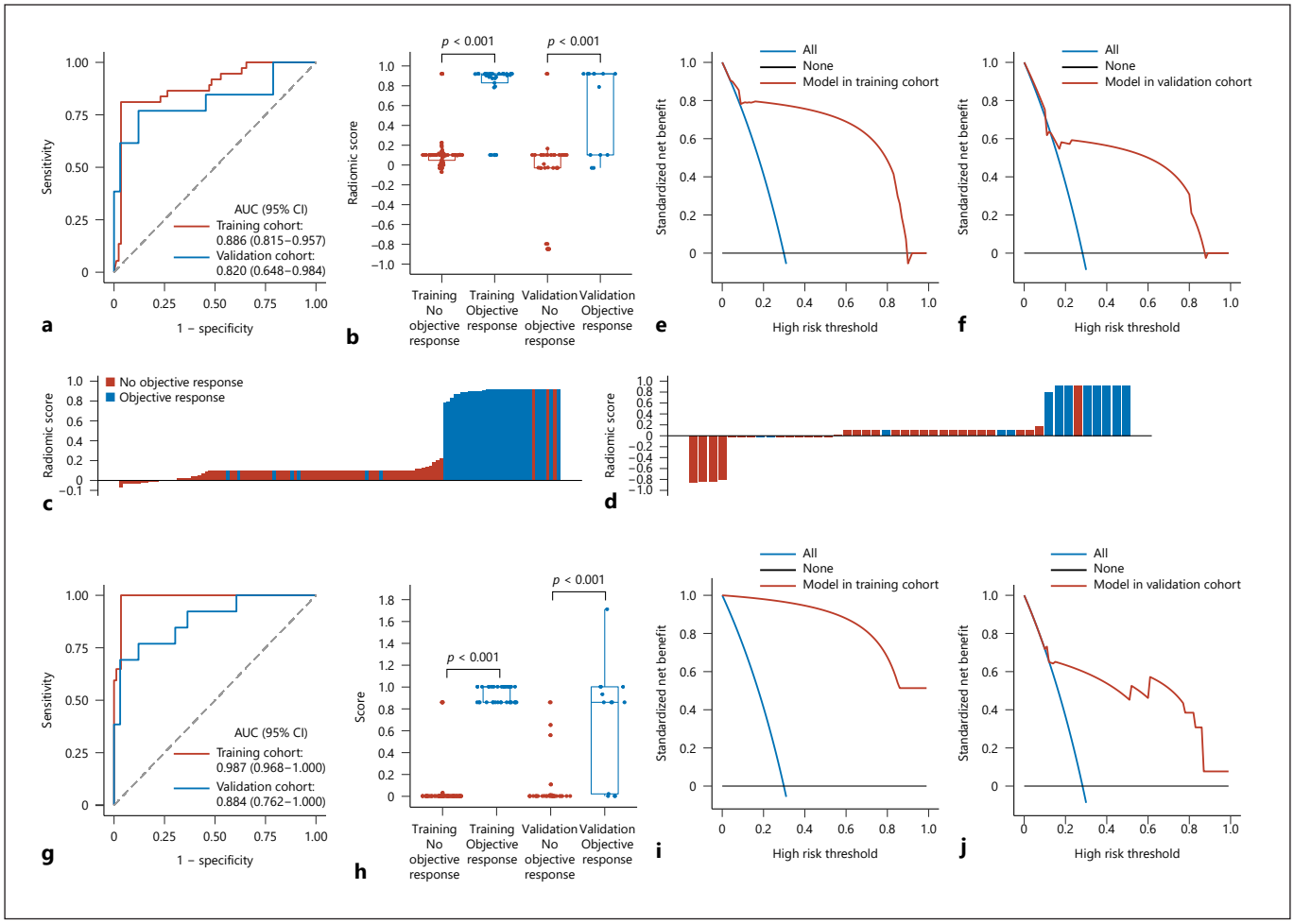

Fig. 3. Performance of the radiomic and clinicopathologic-radiomic models. **a** The ROC of radiomic model in the training and validation cohorts. **b** The scores predicted by radiomic model between patients with and without objective response in the training and validation cohorts. **c**, **d** The radiomic score of each patient in the training cohort and validation cohort, respectively. **e**, **f** The decision curves of radiomic model in the training cohort and validation cohort, respectively. **g** The ROC of clinicopathologic-radiomic model in the training and validation cohorts. **h** The scores predicted by clinicopathologic-radiomic model between patients with and without objective response in the training and validation cohorts. **i**, **j** The decision curves of clinicopathologic-radiomic model in the training cohort and validation cohort, respectively. AUC, area under the receiver operating characteristic curve; CI, confidence intervals; ROC, receiver operating characteristic curve.

the training and validation cohorts (online suppl. Table S6).

Rad-scores were significantly associated with objective tumor response both in the training and validation cohorts ($p < 0.001$ for both, Fig. 3b; the distributions of rad-scores in the training and validation cohorts are shown in Fig. 3c, d, respectively). The optimal cut-off threshold of rad-score was 0.504, and accuracy, sensitivity, specificity, PPV, and NPV for the radiomic model are summarized in Table 3. Patients with a rad-score >0.504 were predicted to have an objective response; otherwise, patients were predicted not to have an objective response. This cut-off discriminated between patients with and without an objective response in both the training and validation cohorts ($p < 0.001$ for both, Table 4).

There were no statistically significant differences in the clinicopathologic features between patients predicted to have an objective response and those predicted not to in the training cohort (online suppl. Table S7). Compared with patients predicted not to have an objective response in the validation cohort, a smaller proportion of patients predicted to have an objective response were AFP >400 ng/mL (11.1% vs. 59.5%, $p = 0.022$), and they had an earlier CNLC stage ($p = 0.011$) (online suppl. Table S8). The cali-

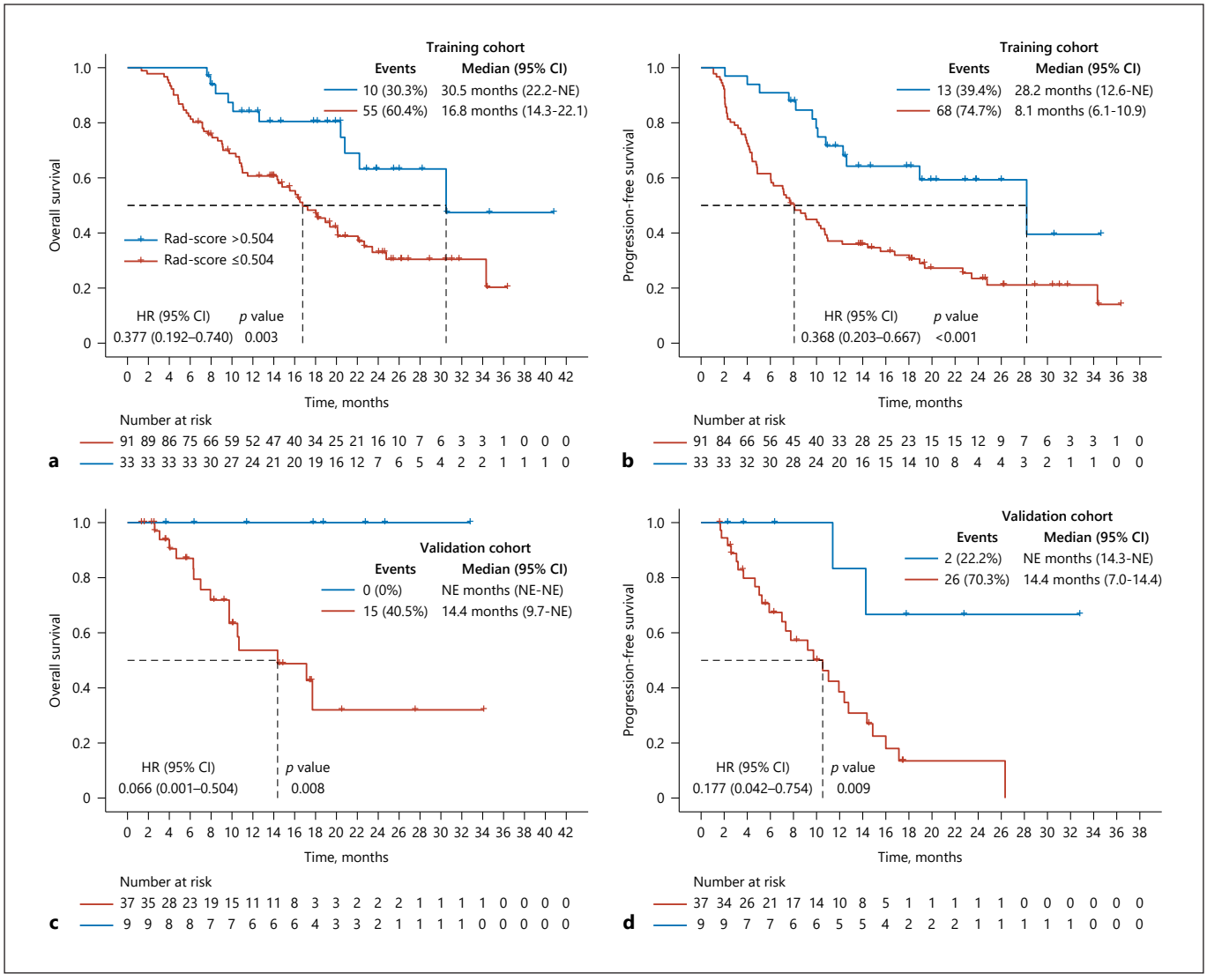

Fig. 4. Association between radiomics features and overall survival/progression-free survival. **a**, **b** Association between radiomics features and overall survival/progression-free survival in the training cohorts. **c**, **d** Association between radiomics features and overall survival/progression-free survival in the validation cohorts. CI, confidence interval; HR, hazard ratio; NE, not evaluable; rad-score, radiomic score.

bration curves showed good agreement between the outcomes predicted by the radiomic model and the actual clinical outcomes (online suppl. Fig. S5). The decision curves revealed that the radiomic prediction model can add net benefit than assuming all patients did or did not have an objective response in both the training and validation cohorts (Fig. 3e, f). These results demonstrated that radiomic features obtained from pretreatment MRI can predict objective response to lenvatinib plus an anti-PD-1 antibody with good discrimination, calibration, and clinical utility, independent on clinicopathologic features.

Incremental Predictive Value of Radiomic Features over Clinicopathologic Features

We incorporated rad-scores calculated using the radiomic model into the clinicopathologic model and built a clinicopathologic-radiomic model with 5, 3, and 2 neurons in the hidden layers 1, 2, and 3, respectively. The diagram and formula of this model are shown in online supplementary Figure S6. The AUC (95% CI) using this model was 0.987 (0.968–1.000) and 0.884 (0.762–1.000) in the training and validation cohorts, respectively, after bootstrap resampling (n = 1,000) (Fig. 3g).

The scores calculated using the clinicopathologic-radiomic model were significantly associated with objective tumor response in both the training and validation cohorts ($p < 0.001$ for both; Fig. 3h). The optimal cut-off for this model was 0.443, and accuracy, sensitivity, specificity, PPV, and NPV for this model are summarized in Table 3. Patients with a score >0.443 were predicted to have an objective response; otherwise, patients were predicted not to have an objective response. This cut-off threshold discriminated between patients with and without an objective response in both the training and validation cohorts ($p < 0.001$ for both, Table 4). The calibration curves showed good agreement between the outcomes predicted by clinicopathologic-radiomic model and the actual clinical outcomes (online suppl. Fig. S5). The decision curves revealed that this prediction model can add net benefit than assuming all patients did or did not have an objective response in both the training and validation cohorts (Fig. 3i, j).

Compared with the clinicopathologic model, the clinicopathologic-radiomic model had a higher AUC in the training cohort (0.987 vs. 0.748, $p < 0.001$) and a marginally higher AUC in the validation cohort (0.884 vs. 0.702, $p = 0.074$). According to NRI, the clinicopathologic-radiomic model improved prediction performance over the clinicopathologic model in both the training (NRI = 47.9%, $p < 0.001$) and validation cohorts (NRI = 41.5%, $p = 0.025$). These results indicated that radiomic features can provide incremental predictive value to clinicopathologic features for prediction of objective response to lenvatinib plus an anti-PD-1 antibody.

Radiomic Features Associated with OS and PFS

As of August 22, 2022, median follow-up was 15.2 (IQR: 8.5–22.2) months in the training cohort and 10.0 (IQR: 4.4–17.6) months in the validation cohort; median duration of treatment was 5.6 (IQR: 2.5–9.0) months in the training cohort and 6.0 (IQR: 2.6–14.8) months in the validation cohort. 81 (65.3%) of 124 patients in the training cohort and 28 (60.9%) of 46 patients in the validation cohort had progressive disease or died. The median OS was 20.1 (95% CI: 16.8–30.5) months in the training cohort and was not reached in the validation cohort; the median PFS was 10.7 (95% CI: 8.2–18.0) months and 11.4 (95% CI: 9.2–16.0) months in the training and validation cohorts, respectively (online suppl. Fig. S7).

Patients with a rad-score >0.504 were associated with a significantly longer median OS or median PFS than those with a rad-score ≤0.504 both in the training cohort (median OS: 30.5 (95% CI: 22.2–not evaluable (NE)) months versus 16.8 (95% CI: 14.3–22.1) months, hazard ratio (HR) (95% CI): 0.377 (0.192–0.740), $p = 0.003$; median PFS: 28.2 (95% CI: 12.6–NE) months versus 8.1 (95% CI: 6.1–10.9) months, HR (95% CI): 0.368 (0.203–0.667), $p < 0.001$) and validation cohort (median OS: NE (95% CI: NE–NE) months versus 14.4 (95% CI: 9.7–NE) months, HR (95% CI): 0.066 (0.001–0.504), $p = 0.008$; median PFS: NE (95% CI: 14.3–NE) months versus 10.5 (95% CI: 7.0–14.4) months, HR (95% CI): 0.177 (0.042–0.754), $p = 0.009$; Fig. 4).

Previous studies showed that modified albumin-bilirubin (mALBI) grade [36, 37] and neutrophil-to-lymphocyte ratio (NLR) [38] were associated with OS and PFS in lenvatinib treatment. In the drug combination setting of this study, mALBI grade was associated with OS in the training cohort ($p = 0.018$) but not in the validation cohort ($p = 0.360$); mALBI grade was not associated with PFS both in the training ($p = 0.570$) and validation ($p = 0.270$) cohorts (online suppl. Fig. S8).

The AUC (95% CI) using NLR to predict objective response was 0.514 (0.404–0.623) and 0.629 (0.400–0.826) in the training and validation cohorts, respectively, after bootstrap resampling ($n = 1{,}000$). The optimal cut-off threshold of NLR was 5.861 by Youden index using ROC. NLR was not associated with OS or PFS both in the training and validation cohorts (online suppl. Fig. S9). When using 2.548 (the median value of NLR) as the optimal cut-off threshold, NLR was not associated with OS in the training cohort ($p = 0.095$) but in the validation cohort ($p = 0.014$); NLR was not associated with PFS both in the training ($p = 0.440$) and validation ($p = 0.350$) cohorts (online suppl. Fig. S10). When using 3 [38] as the optimal cut-off threshold, NLR was associated with OS both in the training (HR (95% CI): 0.568 (0.347–0.929), $p = 0.022$) and validation (HR (95% CI): 0.291 (0.102–0.824), $p = 0.014$) cohorts, but not associated with PFS both in the training ($p = 0.470$) and validation ($p = 0.380$) cohorts (online suppl. Fig. S11).

Discussion

In this study, we developed a radiomic model based on pretreatment MRI to predict objective responses to combination therapy with lenvatinib plus an anti-PD-1 antibody in patients with unresectable or advanced HCC, which was validated in a multicenter dataset, and indicated that radiomic features were associated with OS and PFS after initiating this combination therapy. To the best of our knowledge, this is the first study to report the radiomic analysis based on pretreatment contrast-enhanced

MRI to predict response to combination therapy with lenvatinib plus an anti-PD-1 antibody in advanced HCC patients.

Tumor radiomic features were associated with response to anti-PD-1 antibodies or lenvatinib monotherapy plus TACE in advanced HCC in two recent studies [39, 40], providing important data to support the generation of the hypothesis of the present study. The first study proposed a radiomic model based on contrast-enhanced CT with a relatively small sample size ($N = 58$) from one center to predict response to anti-PD-1 antibodies monotherapy [39]. MRI has several advantages over CT; it can provide superior contrast resolution, does not rely on ionizing radiation [41], and remains the preferred modality to assess response to systemic therapy in HCC [28]. In the second study, tumor radiomic features extracted from pretreatment MRI predicted disease progression after lenvatinib monotherapy plus TACE [40]. It was also a single-center study with a small sample size ($N = 61$); the AUC was 0.71, which had a modest discrimination power.

All (17/17) the final radiomic features selected to predict objective response were from wavelet and Laplacian of Gaussian filtered images instead of original images, indicating that radiomics can be used to identify details and extract features on MRI that cannot be captured or quantified by the naked eye, and thus accurately reflect the biology of HCC. These high-dimensional features cannot be detected in original images or by the naked eye, but hold more detailed information about the tumors and more sensitively predicted treatment response than clinicopathologic features [24]. For example, the "3D_glszm_GrayLevelVariance" feature represents the discrete degree of gray level in tumor regions, which was associated with tumor heterogeneity (e.g., tumor cellularity, micro-necrosis, and inflammation). Previous studies have shown that tumor heterogeneity is related to tumor response, which is consistent with the results of this study [42, 43]. Furthermore, the "firstorder_Kurtosis" feature was associated the degree of tumor enhancement in the arterial phase, which reflects tumor vasculature. A previous study has shown that the enhancement degree of tumor in arterial phase before immunotherapy is related to its progression [44]. The remaining texture features may reflect the immune microenvironment of tumors, but need to be further studied with genomic or histological correlative data [31].

Consistent with the present study, the model based on clinicopathologic features alone did not satisfactorily predict objective response; however, the radiomic model robustly predicted objective response. Furthermore, incorporating radiomic features into the clinicopathologic model provided incremental predictive value for objective response, suggesting that clinicopathologic features and radiomic features may reflect different characteristics of tumors related to the response to combination therapy. The clinicopathologic-radiomic model had a marginally higher AUC than the clinicopathologic model (0.884 vs. 0.702, $p = 0.074$) in the validation cohort, which may be attributed to an insufficient sample size. However, using NRI, we confirmed the incremental predictive value of radiomic features compared with clinicopathologic features in predicting response. Tumor radiomic features may capture tumor biology and heterogeneity; however, the objective response is not only associated with tumor biology but also related to tumor burden and condition of patients. For example, according to the updated IMbrave150 data, patients with BCLC stage B disease had a higher objective response than all patients (43.0% vs. 29.8%) [45, 46]. Therefore, the clinicopathologic-radiomic model provided a modestly higher discriminative ability to predict the objective response than the radiomic model in each cohort.

As the prognosis of HCC patients depends on tumor burden and hepatic reserve function, previous studies demonstrated that the mALBI grade was a negative prognostic factor for OS in lenvatinib treatment against advanced HCC [36, 37]. However, mALBI grade was only associated with OS in the training cohort, but not in validation cohort, which might be attributed to limited patient number and immature survival data in the validation cohort, or different treatment regimen. Another study first indicated NLR <3 was a favorable factor for OS in HCC patients treated with lenvatinib [38]. In this study, NLR <3 was demonstrated to be associated with OS both in the training and validation cohorts for lenvatinib plus an anti-PD-1 antibody, but not associated with PFS.

This study has several limitations. First, it had a limited sample size with potential selection bias. The sample size requirement for developing the radiomic model in the training cohort was met, but more data are required to optimize and improve models. Second, the majority of the study population had hepatitis B virus-related HCC. As heterogeneity exists in patients with HCC of different etiologies [47], the proposed radiomic model may not be applied to HCC patients with nonalcoholic fatty liver disease or infected with hepatitis C virus. Additional studies are required to compare the differences in radiomic features among patients with HCC of different etiologies. Third, due to the retrospective nature of this

study, the MR image acquisition parameters were not standardized across different hospitals, although this study demonstrated that MR image preprocessing could overcome this influence; furthermore, tumor tissues were not prospectively collected to explore the biological meaning of radiomic features. Fourth, manual segmentation of tumors is relatively subjective, especially for tumors with blurry edges, but ICC was used to reduce subjectivity and ensure robustness and reproducibility as previously reported [31]. Automatic or semiautomatic segmentation tools may reduce the interobserver ICC. Furthermore, only radiomic features from arterial and delayed phases were analyzed. Although characteristics of HCC on imaging are mainly reflected on these two phases, radiomic features from other sequences in MRI should be analyzed in the future. Fifth, different anti-PD-1 antibodies were used across the study population, which could increase internal variability with a limited sample size; however, lenvatinib in combination with different anti-PD-1 antibodies were reported to have similar ORRs [6] and could reflect real-world practice.

In conclusion, this study demonstrated that tumor radiomic features extracted from pretreatment MRI can be used to predict objective response to combination therapy with lenvatinib plus an anti-PD-1 antibody in patients with unresectable or advanced HCC, and provide incremental predictive value over clinicopathologic features, and are associated with OS and PFS after initiation of this combination regimen. A prospective study with a unified protocol to investigate the performance of radiomic and clinicopathologic-radiomic models and to explore their usage in patients receiving existing first-line systemic treatments for advanced HCC is warranted.

Acknowledgments

We thank the patients and their families. We also thank the China liver cancer study group young investigators (CLEAP) for their joint efforts for this work.

Statement of Ethics

The study protocol was conducted in accordance with the principles of the World Medical Association Declaration of Helsinki and was approved by the Zhongshan Hospital Research Ethics Committee (Approval Numbers: B2021-210). The requirement for informed consent was waived (retrospective computational analysis of images) by the Zhongshan Hospital Research Ethics Committee.

Conflict of Interest Statement

Hui-Chuan Sun has received honorarium or lecture fees from Roche, Bayer, MSD, Eisai, Hengrui, Innovent, TopAlliance, Abbott, Beigene, Gilead, and Zelgen during the last 5 years. Jia Fan is an Editorial Board Member of Liver Cancer. All remaining authors have no conflicts of interest to declare.

Funding Sources

This work was supported by the Leading Investigator Program of the Shanghai municipal government (17XD1401100), the National Key Basic Research Program (973 Program, 2015CB554005) from the Ministry of Science and Technology of China, the National Natural Science Foundation of China (81871928), the Special Research Fund for Liver Cancer Diagnosis and Treatment from the China Anti-Cancer Association (H2020-008), and the Clinical Research Special Fund of Zhongshan Hospital, Fudan University (2020ZSLC71) to Hui-Chuan Sun.

Author Contributions

Study concept and design, drafting of the manuscript: Bin Xu and Hui-Chuan Sun; acquisition of data: Bin Xu, San-Yuan Dong, Xue-Li Bai, Tian-Qiang Song, Bo-Heng Zhang, Le-Du Zhou, Yong-Jun Chen, Zhi-Ming Zeng, Kui Wang, Hai-Tao Zhao, Na Lu, Wei Zhang, Xu-Bin Li, Su-Su Zheng, Guo Long, Yu-Chen Yang, Hua-Sheng Huang, Lan-Qing Huang, Yun-Chao Wang, Xiao-Dong Zhu, Cheng Huang and Ying-Hao Shen; analysis and interpretation of data and critical revision of the manuscript for important intellectual content: all authors; statistical analysis: Bin Xu, San-Yuan Dong, Fei Liang and Hui-Chuan Sun; obtained funding: Hui-Chuan Sun; administrative, technical, or material support, study supervision: Xue-Li Bai, Tian-Qiang Song, Bo-Heng Zhang, Le-Du Zhou, Yong-Jun Chen, Zhi-Ming Zeng, Kui Wang, Hai-Tao Zhao, Jian Zhou, Meng-Su Zeng, Jia Fan, Sheng-Xiang Rao, and Hui-Chuan Sun.

Data Availability Statement

Raw data of MRI used in this study are unable to be shared as the requirement of Hospital Research Ethics Committees. Derived data (e.g., extracted radiomic features) are available upon reasonable request from the corresponding authors.

References

1 Sung H, Ferlay J, Siegel RL, Laversanne M, Soerjomataram I, Jemal A, et al. Global cancer statistics 2020: GLOBOCAN estimates of incidence and mortality worldwide for 36 cancers in 185 countries. CA Cancer J Clin. 2021;71(3):209–49.

2 Zheng R, Zhang S, Zeng H, Wang S, Sun K, Chen R, et al. Cancer incidence and mortality in China, 2016. J Natl Cancer Cent. 2022;2(1):1–9.

3 Park J-W, Chen M, Colombo M, Roberts LR, Schwartz M, Chen P-J, et al. Global patterns of hepatocellular carcinoma management from diagnosis to death: the BRIDGE Study. Liver Int. 2015;35(9):2155–66.
4 Ren Z, Xu J, Bai Y, Xu A, Cang S, Du C, et al. Sintilimab plus a bevacizumab biosimilar (IBI305) versus sorafenib in unresectable hepatocellular carcinoma (ORIENT-32): a randomised, open-label, phase 2-3 study. Lancet Oncol. 2021;22(7):977–90.
5 Finn RS, Ikeda M, Zhu AX, Sung MW, Baron AD, Kudo M, et al. Phase Ib study of lenvatinib plus pembrolizumab in patients with unresectable hepatocellular carcinoma. J Clin Oncol. 2020;38(26):2960–70.
6 Huang C, Zhu X-D, Shen Y-H, Wu D, Ji Y, Ge N-L, et al. Organ specific responses to first-line lenvatinib plus anti-PD-1 antibodies in patients with unresectable hepatocellular carcinoma: a retrospective analysis. Biomark Res. 2021;9(1):19.
7 Finn RS, Kudo M, Merle P, Meyer T, Qin S, Ikeda M, et al. LBA34 - primary results from the phase III LEAP-002 study: lenvatinib plus pembrolizumab versus lenvatinib as first-line (1L) therapy for advanced hepatocellular carcinoma (aHCC). Ann Oncol. 2022;33(suppl_7):S1401–69.
8 Zhu X-D, Huang C, Shen Y-H, Ji Y, Ge N-L, Qu X-D, et al. Downstaging and resection of initially unresectable hepatocellular carcinoma with tyrosine kinase inhibitor and anti-PD-1 antibody combinations. Liver Cancer. 2021;10:320–9.
9 Zhang W, Hu B, Han J, Wang Z, Ma G, Ye H, et al. Surgery after conversion therapy with PD-1 inhibitors plus tyrosine kinase inhibitors are effective and safe for advanced hepatocellular carcinoma: a pilot study of ten patients. Front Oncol. 2021;11:747950.
10 Zhu X-D, Huang C, Shen Y-H, Xu B, Ge N-L, Ji Y, et al. Hepatectomy after conversion therapy using tyrosine kinase inhibitors plus anti-PD-1 antibody therapy for patients with unresectable hepatocellular carcinoma. Ann Surg Oncol. 2022.
11 Xu B, Zhu X-D, Huang C, Shen Y-H, Zhu J-J, Li M-L, et al. Clinical efficacy of combination therapy with lenvatinib and programmed death-1 antibodies in unresectable or advanced hepatocellular carcinoma. Chin J Dig Surg. 2021;20(02):197–204.
12 Cheng A-L, Hsu C, Chan SL, Choo S-P, Kudo M. Challenges of combination therapy with immune checkpoint inhibitors for hepatocellular carcinoma. J Hepatol. 2020;72(2):307–19.
13 Luchini C, Bibeau F, Ligtenberg MJL, Singh N, Nottegar A, Bosse T, et al. ESMO recommendations on microsatellite instability testing for immunotherapy in cancer, and its relationship with PD-1/PD-L1 expression and tumour mutational burden: a systematic review-based approach. Ann Oncol. 2019;30(8):1232–43.
14 Meric-Bernstam F, Larkin J, Tabernero J, Bonini C. Enhancing anti-tumour efficacy with immunotherapy combinations. Lancet. 2021;397(10278):1010–22.
15 Lambin P, Leijenaar RTH, Deist TM, Peerlings J, de Jong EEC, van Timmeren J, et al. Radiomics: the bridge between medical imaging and personalized medicine. Nat Rev Clin Oncol. 2017;14(12):749–62.
16 Gillies RJ, Kinahan PE, Hricak H. Radiomics: images are more than pictures, they are data. Radiology. 2016;278(2):563–77.
17 Gao R, Zhao S, Aishanjiang K, Cai H, Wei T, Zhang Y, et al. Deep learning for differential diagnosis of malignant hepatic tumors based on multi-phase contrast-enhanced CT and clinical data. J Hematol Oncol. 2021;14(1):154.
18 Kim S, Shin J, Kim D-Y, Choi GH, Kim M-J, Choi J-Y. Radiomics on gadoxetic acid–enhanced magnetic resonance imaging for prediction of postoperative early and late recurrence of single hepatocellular carcinoma. Clin Cancer Res. 2019;25(13):3847–55.
19 Wu L-F, Rao S-X, Xu P-J, Yang L, Chen C-Z, Liu H, et al. Pre-TACE kurtosis of ADCtotal derived from histogram analysis for diffusion-weighted imaging is the best independent predictor of prognosis in hepatocellular carcinoma. Eur Radiol. 2019;29(1):213–23.
20 Yang L, Gu D, Wei J, Yang C, Rao S, Wang W, et al. A radiomics nomogram for preoperative prediction of microvascular invasion in hepatocellular carcinoma. Liver Cancer. 2019;8(5):373–86.
21 Xu X, Zhang H-L, Liu Q-P, Sun S-W, Zhang J, Zhu F-P, et al. Radiomic analysis of contrast-enhanced CT predicts microvascular invasion and outcome in hepatocellular carcinoma. J Hepatol. 2019;70(6):1133–44.
22 Kong C, Zhao Z, Chen W, Lv X, Shu G, Ye M, et al. Prediction of tumor response via a pretreatment MRI radiomics-based nomogram in HCC treated with TACE. Eur Radiol. 2021;31(10):7500–11.
23 Liu Z, Zhang X-Y, Shi Y-J, Wang L, Zhu H-T, Tang Z, et al. Radiomics analysis for evaluation of pathological complete response to neoadjuvant chemoradiotherapy in locally advanced rectal cancer. Clin Cancer Res. 2017;23(23):7253–62.
24 Liu Z, Li Z, Qu J, Zhang R, Zhou X, Li L, et al. Radiomics of multiparametric MRI for pretreatment prediction of pathologic complete response to neoadjuvant chemotherapy in breast cancer: a multicenter study. Clin Cancer Res. 2019;25(12):3538–47.
25 Dercle L, Fronheiser M, Lu L, Du S, Hayes W, Leung DK, et al. Identification of non-small cell lung cancer sensitive to systemic cancer therapies using radiomics. Clin Cancer Res. 2020;26(9):2151–62.
26 Sun R, Limkin EJ, Vakalopoulou M, Dercle L, Champiat S, Han SR, et al. A radiomics approach to assess tumour-infiltrating CD8 cells and response to anti-PD-1 or anti-PD-L1 immunotherapy: an imaging biomarker, retrospective multicohort study. Lancet Oncol. 2018;19(9):1180–91.
27 Ligero M, Garcia-Ruiz A, Viaplana C, Villacampa G, Raciti MV, Landa J, et al. A CT-based radiomics signature is associated with response to immune checkpoint inhibitors in advanced solid tumors. Radiology. 2021;299(1):109–19.
28 Lencioni R, Llovet JM. Modified RECIST (mRECIST) assessment for hepatocellular carcinoma. Semin Liver Dis. 2010;30(1):52–60.
29 Zhou J, Sun H, Wang Z, Cong W, Wang J, Zeng M, et al. Guidelines for the diagnosis and treatment of hepatocellular carcinoma (2019 edition). Liver Cancer. 2020;9(6):682–720.
30 Bruix J, Sherman M, American Association for the Study of Liver Diseases. Management of hepatocellular carcinoma: an update. Hepatology. 2011;53(3):1020–2.
31 Dong D, Fang M-J, Tang L, Shan X-H, Gao J-B, Giganti F, et al. Deep learning radiomic nomogram can predict the number of lymph node metastasis in locally advanced gastric cancer: an international multicenter study. Ann Oncol. 2020;31(7):912–20.
32 van Griethuysen JJM, Fedorov A, Parmar C, Hosny A, Aucoin N, Narayan V, et al. Computational radiomics system to decode the radiographic phenotype. Cancer Res. 2017;77(21):e104–7.
33 Collins GS, Reitsma JB, Altman DG, Moons KGM. Transparent reporting of a multivariable prediction model for individual prognosis or diagnosis (TRIPOD): the TRIPOD statement. Ann Intern Med. 2015;162(1):55–63.
34 Leening MJG, Vedder MM, Witteman JCM, Pencina MJ, Steyerberg EW. Net reclassification improvement: computation, interpretation, and controversies: a literature review and clinician's guide. Ann Intern Med. 2014;160(2):122–31.
35 Fitzgerald M, Saville BR, Lewis RJ. Decision curve analysis. JAMA. 2015;313(4):409–10.
36 Hiraoka A, Kumada T, Atsukawa M, Hirooka M, Tsuji K, Ishikawa T, et al. Prognostic factor of lenvatinib for unresectable hepatocellular carcinoma in real-world conditions—multicenter analysis. Cancer Med. 2019;8(8):3719–28.
37 Hiraoka A, Kumada T, Atsukawa M, Hirooka M, Tsuji K, Ishikawa T, et al. Important clinical factors in sequential therapy including lenvatinib against unresectable hepatocellular carcinoma. Oncology. 2019;97(5):277–85.
38 Rimini M, Shimose S, Lonardi S, Tada T, Masi G, Iwamoto H, et al. Lenvatinib versus Sorafenib as first-line treatment in hepatocellular carcinoma: a multi-institutional matched case-control study. Hepatol Res. 2021;51(12):1229–41.
39 Yuan G, Song Y, Li Q, Hu X, Zang M, Dai W, et al. Development and validation of a contrast-enhanced CT-based radiomics nomogram for prediction of therapeutic efficacy of anti-PD-1 antibodies in advanced HCC patients. Front Immunol. 2020;11:613946.

40 Luo J, Huang Z, Wang M, Li T, Huang J. Prognostic role of multiparameter MRI and radiomics in progression of advanced unresectable hepatocellular carcinoma following combined transcatheter arterial chemoembolization and lenvatinib therapy. BMC Gastroenterol. 2022;22(1):108.
41 Vu LN, Morelli JN, Szklaruk J. Basic MRI for the liver oncologists and surgeons. J Hepatocell Carcinoma. 2017;5:37–50.
42 Sun R, Limkin EJ, Vakalopoulou M, Dercle L, Champiat S, Han SR, et al. A radiomics approach to assess tumour-infiltrating CD8 cells and response to anti-PD-1 or anti-PD-L1 immunotherapy: an imaging biomarker, retrospective multicohort study. Lancet Oncol. 2018;19(9):1180–91.
43 Dercle L, Lu L, Schwartz LH, Qian M, Tejpar S, Eggleton P, et al. Radiomics response signature for identification of metastatic colorectal cancer sensitive to therapies targeting EGFR pathway. J Natl Cancer Inst. 2020;112(9):902–12.
44 Sheng R, Zeng M, Jin K, Zhang Y, Wu D, Sun H. MRI-Based nomogram predicts the risk of progression of unresectable hepatocellular carcinoma after combined lenvatinib and anti-PD-1 antibody therapy. Acad Radiol. 2022;29(6):819–29.
45 Finn RS, Qin S, Ikeda M, Galle PR, Ducreux M, Kim T-Y, et al. IMbrave150: updated overall survival (OS) data from a global, randomized, open-label phase III study of atezolizumab (atezo) + bevacizumab (bev) versus sorafenib (sor) in patients (pts) with unresectable hepatocellular carcinoma (HCC). J Clin Oncol. 2021;39(3 suppl):267.
46 Kudo M, Finn RS, Galle PR, Zhu A, Ducreux MP, Cheng A-L, et al. 932P IMbrave150: exploratory efficacy and safety results in patients with hepatocellular carcinoma without macrovascular invasion (MVI) or extrahepatic spread (EHS) treated with atezolizumab (atezo) + bevacizumab (bev) or sorafenib (sor). Ann Oncol. 2021;32:S818.
47 Barcena-Varela M, Lujambio A. The endless sources of hepatocellular carcinoma heterogeneity. Cancers. 2021;13(11):2621.